



Design of a compact LPF and a miniaturized Wilkinson power divider using aperiodic stubs with harmonic suppression for wireless applications

Saeed Roshani¹ · Sobhan Roshani¹

Published online: 13 December 2019
© Springer Science+Business Media, LLC, part of Springer Nature 2019

Abstract

In this paper a miniaturized low pass filter (LPF) with 2.5 GHz cut-off frequency and a novel compact, harmonics suppressed Wilkinson power divider (WPD) at 0.7 GHz is proposed. The proposed divider consists of two multi-stub LPFs and three open stubs at each port. The presented open stub at port one suppresses the second harmonic and other two open stubs at output ports, suppress the third harmonic. To suppress high order harmonics a novel 12 sections LPF based on aperiodic stub is proposed. This filter is designed to suppress 4th to 15th harmonics. The cut off frequency of applied filter is 2.5 GHz, which creates 12 transmission zeros and suppresses corresponding 4th–15th harmonics of the proposed divider. The proposed WPD not only has perfect harmonics suppression, but also extremely decreases the circuit size. The overall size of the fabricated divider is only $0.116 \lambda_g \times 0.044 \lambda_g$, which shows more than 73% size reductions, compared to the 0.7 GHz conventional WPD.

Keywords Aperiodic stubs · Harmonic suppression · Low pass filter · Wilkinson power divider · Wireless communication

1 Introduction

Power dividers are widely used in the wireless communication circuits and microwave applications, such as array antennas, phase shifters, modulators, power amplifiers, mixers and frequency multipliers for power division or combination [1–3]. The conventional Wilkinson power divider (WPD) occupies considerably large area and suffers from presence of unwanted harmonics in the frequency response [4–6]. So far, several methods have been presented for harmonic suppression and size reduction in microwave circuits [7–10].

In [11, 12] the electronic band gap structure, in [13, 14] the defected ground structure and in [15] lumped reactive elements (capacitance and inductance) are applied to miniaturize and suppress unwanted harmonics, which all of

these structures are not desirable, because of etching process or additional lumped reactive components [1].

In [16–21] resonators are used to suppress unwanted harmonics. Unfortunately, applying resonators resulted in insertion loss increment in passband and more complex design.

In [22–27] open shunt stubs are applied to improve performance of power dividers. The open shunt stubs are the most common configuration of microstrip structure [23], which applied for various purposes, such as: impedance matching [24], harmonics suppression [25] and size reduction [27].

So far, in several approaches, open stubs are presented to design the power divider, but just a few works have utilized aperiodic stubs methods. Aperiodic stubs are applied in [23, 28] to design artificial transmission line (ATL) and LPF.

In some recent works [29, 30] coupled lines are applied to suppress unwanted harmonics, which in this method the insertion loss parameter is poor.

In the proposed paper, aperiodic stubs are applied to design a miniaturized and harmonics suppressed Wilkinson power divider (WPD) for the first time. The proposed

✉ Saeed Roshani
s_roshany@yahoo.com

¹ Department of Electrical Engineering, Kermanshah Branch, Islamic Azad University, Kermanshah, Iran

divider has the ability of creating transmission zeros at desired frequencies by using aperiodic stubs. All dimensions of these aperiodic stubs are calculated analytically in the proposed paper. Also, a miniaturized size for the proposed divider is achieved by meandering of the aperiodic stubs lines. The proposed divider works at 700 MHz, which is a candidate band for fifth generation (5G) applications in many countries [31]. 5G networks have been considered as modern communication networks, which can supply high technology applications [32–34]. The performance analysis for small cell networks and transmission problems in wireless local area networks (WLANs) for 5G operating frequency bands are completely discussed in [35–37].

In the following sections, circuit analysis of the open stubs is presented in Sect. 2. The proposed 12 sections low pass filter (LPF) is based on aperiodic open stubs to suppress 12 unwanted harmonics (4th–15th), which is designed in Sect. 3. In Sect. 4, design process of the proposed Wilkinson power divider, consisting of two proposed LPFs and three open stubs at each port, is presented. Simulations and measurements results show that the proposed WPD has good performance.

2 Circuit analysis

The microstrip transmission lines are widely used in microwave circuits. Transmission line can be assumed as cascading of n-section aperiodic lines as depicted in Fig. 1. The electrical length of the transmission line (θ_{0T}) must be equal to sum of n-aperiodic sections with electrical length of θ_{0n} as shown in (1).

$$\theta_{0T} = \theta_{01} + \theta_{02} + \theta_{03} + \dots + \theta_{0n} \tag{1}$$

In low pass filter design, each section can be replaced by T-shaped structure, to reduce the size, as shown in Fig. 2. Each T-shaped structure includes two microstrip lines and an open circuit stub, with same characteristic impedance. T-shaped structure can be used as an ATL with smaller length compared to the conventional line.

Therefore, in many works T-shaped structure are used to decrease the physical length of the conventional transmission line (TL). For example in Fig. 2, the conventional line

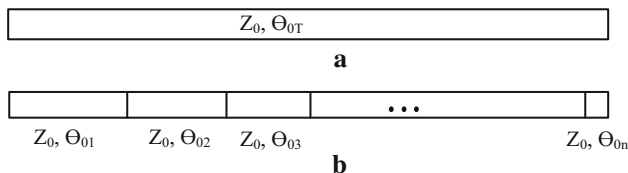


Fig. 1 a Conventional and b aperiodic n-section cascading transmission lines

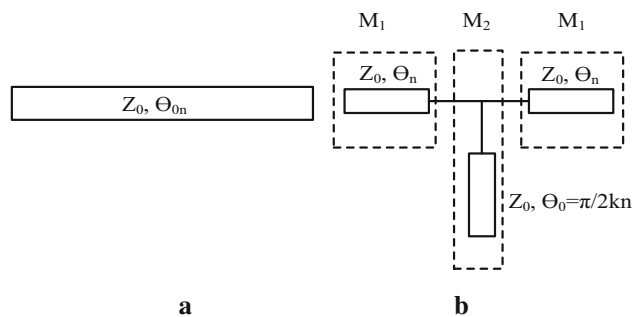


Fig. 2 a Conventional transmission line and b equivalent T-shaped circuit

has the same result with T-shape structure, but the electrical length of the T-shaped structure is shorter than conventional one, which is shown in Eqs. (2) and (3).

$$\theta_{0n} > 2\theta_n \tag{2}$$

$$\theta_{0T} > 2(\theta_1 + \theta_2 + \theta_3 + \dots + \theta_n) \tag{3}$$

The ABCD matrix for the conventional TL, which depicted in Fig. 2a, is given by (4) [24]:

$$\begin{bmatrix} A & B \\ C & D \end{bmatrix} = \begin{bmatrix} \cos\theta_{0n} & jZ_0\sin\theta_{0n} \\ j_0Y_0\sin\theta_{0n} & \cos\theta_{0n} \end{bmatrix} \tag{4}$$

Each T-shaped structure consists of three sections, two microstrip lines and one open circuit stub, as depicted in Fig. 2b. The ABCD matrix is demonstrated by M_1 for microstrip lines and demonstrated by M_2 for open stubs, as shown in (5) and (6) [24]:

$$M_1 = \begin{bmatrix} \cos\theta_n & jZ_0\sin\theta_n \\ j_0Y_0\sin\theta_n & \cos\theta_n \end{bmatrix} \tag{5}$$

$$M_2 = \begin{bmatrix} 1 & 0 \\ j_0Y_0\tan\theta_0 & 1 \end{bmatrix} \tag{6}$$

Therefore the ABCD matrix is calculated as follows for one T-shaped structure (M_T), considering as cascading of three networks:

$$M_T = M_1 \times M_2 \times M_1 \tag{7}$$

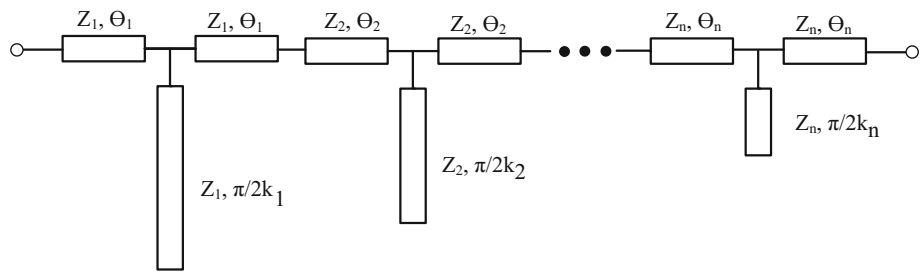
Substituting (5), (6) in (7) resulted in (8):

$$M_T = \begin{bmatrix} \cos^2\theta_n - \sin^2\theta_n - .5\sin 2\theta_n \tan\theta_0 & jZ_0\sin 2\theta_n - jZ_0\sin^2\theta_n \tan\theta_0 \\ j_0Y_0(\sin 2\theta_n + \cos^2\theta_n \tan\theta_0) & \cos^2\theta_n - \sin^2\theta_n - .5\sin 2\theta_n \tan\theta_0 \end{bmatrix} \tag{8}$$

The n-section cascading of T-shaped configuration is depicted in Fig. 3, which known as artificial transmission line and used as low pass filter to suppress n-desired harmonics [23]. Each T-shaped section can suppress a desired harmonic, corresponding to length of the open circuited stub.

In this configuration, the electrical length and characteristic impedance of each T-shaped section is shown with

Fig. 3 Cascading of n-sections T-shaped configuration



θ_m and z_m , respectively. Each T-shaped section creates a specific transmission zero at desired frequency, corresponding to the electrical length of the open circuited stub. The open circuited stub with electrical length of $\pi/2 k_m$ can create a transmission zero at $k_m f_0$ frequency, where f_0 is center frequency, $m = 1, 2, \dots, n$ and k_m is assignable parameter, which specifies the stub length. If k_m is defined as multiplies of center frequency (f_0), then the corresponding harmonic can be suppressed. The electrical length of each two microstrip lines in one T-shaped structure can be calculated as follows:

$$\theta_m = \tan^{-1} \left(\frac{\sqrt{\tan^2 \left(\frac{\pi}{2k_m} \right) + 4 \sin^2 \theta_{0m}} - \tan(\pi/2k_m)}{2 \cos \theta_{0m} + 2} \right) \tag{9}$$

where in (9), θ_m is the electrical length of two microstrip lines in T-shaped structure and θ_{0m} is the electrical length of the conventional transmission line equivalent T-shaped structure. The characteristic impedances of T-shaped structure can be obtained as:

$$Z_m = Z \sqrt{\frac{\cos^2 \theta_m \tan \left(\frac{\pi}{2k_m} \right) + \sin 2\theta_m}{\sin 2\theta_m - \sin^2 \theta_m \tan \left(\frac{\pi}{2k_m} \right)}} \tag{10}$$

All of the characteristic impedance were considered equal ($Z_1 = Z_2 = \dots = Z_n$) in the proposed structure, to minimize the discontinuities and decrease the complexity

of the analysis. To find the unknown design parameters, the equations are defined as below:

$$F_{11} = \theta_0 - \sum_{m=1}^n (\theta_{0m}) \tag{11}$$

and

$$F_{i1} = (Z_1/Z_0) - (Z_i/Z_0)^2 \tag{12}$$

where in (12), $i = 2, 3, \dots, n$. So, the constructed equations involve n-equations. The desired electrical length at the operating frequency of f_0 is demonstrated by θ_0 in (11) and $\theta_{01}, \theta_{02}, \dots, \theta_{0n}$ are the n-unknown variables. To find $\theta_{01}, \theta_{02}, \dots, \theta_{0n}$ variables, unknown parameters of $Z_1/Z_0, Z_2/Z_0, \dots, Z_n/Z_0$, in (12) can be written as $\theta_{01}, \theta_{02}, \dots, \theta_{0n}$, using (9) and (10). As results $\theta_{01}, \theta_{02}, \dots, \theta_{0n}$ are determined. After this step, the values of $\theta_1, \theta_2, \dots, \theta_n$ and Z_1 can be calculated using (9) and (10). The Newton’s method is used to find the answer of this equation with several variables. The solution to the problem of $F = [0 \ 0 \ \dots \ 0]^T$ is formulated as an iterative process

$$X_{i+1} = X_i - J^{-1}F \tag{13}$$

where X in (13) is equal to $[\theta_{01} \ \theta_{02} \ \dots \ \theta_{0n}]^T$. The Jacobian matrix is defined in (14)–(16), with the initial guess of $X^0 = [1^\circ \ 1^\circ \ \dots \ 1^\circ]^T$ can be calculated as follows: Using (10)–(16) allows one to synthesize the value of unknown parameters. More detail about analysis and methods of finding unknown parameter are completely described in [23].

$$J = \begin{bmatrix} -1 & -1 & -1 & -1 & \dots & -1 \\ \frac{\partial(Z_1/Z_0)^2}{\partial\theta_1} \frac{\partial\theta_1}{\partial\theta_{01}} & -\frac{\partial(Z_2/Z_0)^2}{\partial\theta_2} \frac{\partial\theta_2}{\partial\theta_{02}} & 0 & 0 & \dots & 0 \\ \vdots & 0 & -\frac{\partial(Z_3/Z_0)^2}{\partial\theta_3} \frac{\partial\theta_3}{\partial\theta_{03}} & 0 & \dots & 0 \\ \vdots & 0 & 0 & -\frac{\partial(Z_4/Z_0)^2}{\partial\theta_4} \frac{\partial\theta_4}{\partial\theta_{04}} & \dots & 0 \\ \vdots & \vdots & \vdots & \vdots & \ddots & 0 \\ \frac{\partial(Z_1/Z_0)^2}{\partial\theta_1} \frac{\partial\theta_1}{\partial\theta_{01}} & 0 & 0 & 0 & \dots & -\frac{\partial(Z_n/Z_0)^2}{\partial\theta_n} \frac{\partial\theta_n}{\partial\theta_{0n}} \end{bmatrix} \tag{14}$$

$$\frac{\partial(Z_m/Z_0)^2}{\partial\theta_m} = \frac{2 \tan\left(\frac{\pi}{2k_m}\right) \left[\tan^2 \theta_m + \tan\left(\frac{\pi}{2k_m}\right) - \tan \theta_m - 1 \right]}{(1 + \tan^2 \theta_m) \left[\sin 2\theta_m - \sin^2 \theta_m \tan\left(\frac{\pi}{2k_m}\right) \right]^2} \tag{15}$$

LPF structure. At the end, the designed LPFs are added in the primitive divider. The circuit design flowchart of the proposed divider is shown in Fig. 4, to show the design procedures.

$$\frac{\partial\theta_m}{\partial\theta_m} = \frac{1}{(1 + \tan^2 \theta_m)} \frac{\sin \theta_m \left[4 \cos \theta_m - \tan\left(\frac{\pi}{2k_m}\right) \sqrt{\tan^2\left(\frac{\pi}{2k_m}\right) + 4 \sin^2 \theta_m + \tan^2\left(\frac{\pi}{2k_m}\right) + 4} \right]}{\left[2 \cos \theta_m + 2 \right]^2 \sqrt{\tan^2\left(\frac{\pi}{2k_m}\right) + 4 \sin^2 \theta_m}} \tag{16}$$

3 Design procedure

The proposed Wilkinson power divider consists of two LPFs in branch lines and three open stubs at each port. At first, a conventional power divider at 700 MHz is designed. Then, a primitive divider is designed with three open stubs at each port. This divider only suppresses second and third harmonics. On the other hand, to have more harmonic suppression, the LPFs should be designed. To design the LPFs with harmonic suppression, 12 stubs are added in the

3.1 Design of proposed LPF based on aperiodic stub

In power divider design process, applied low pass filters have a critical role. The proposed divider works at 700 MHz frequency and suppressed fourteen harmonics. The second and third unwanted harmonics are eliminated by applied open stubs at each ports of divider and other twelve harmonics are suppressed by proposed LPF. Therefore the proposed LPF should be designed to suppress

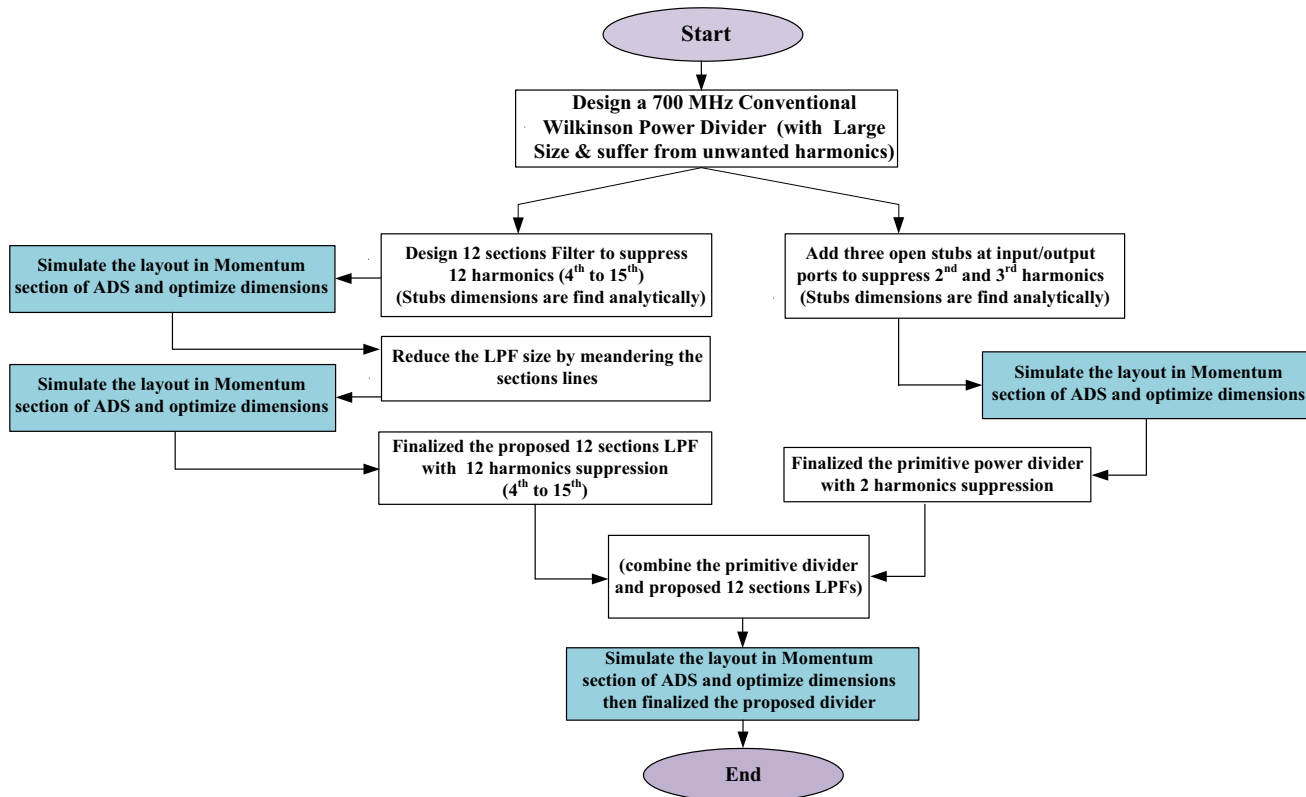


Fig. 4 The circuit design flowchart of the proposed divider

Table 1 Analysis and simulation values of twelve-sections LPF with 142 Ω lines

#	K_m	$2\pi/K_m$ (analysis) (°)	$2\pi/K_m$ (simulation) (°)	Error (%)	θ_{0M} (analysis) (°)	θ_{0M} (simulation) (°)	Error (%)
1	2.8	32.1	32.4	0.9	3.02	3	0.6
2	3.5	25.7	26	1.1	2.6	2.6	0
3	4.2	21.4	21.8	1.8	2.4	2.42	0.8
4	4.9	18.36	18.36	0	2.23	2.24	0.4
5	5.6	16	16.2	1.2	2.12	2.1	0.9
6	6.3	8.7	8.7	0	1.83	1.86	1.6
7	7	7.8	7.6	2.6	1.75	1.77	1.1
8	7.7	6.9	6.9	0	1.64	1.68	2.4
9	8.4	6.3	6.3	0	1.56	1.58	1.2
10	9.1	5.8	5.8	0	1.47	1.5	2
11	9.8	5.4	5.4	0	1.36	1.4	2.8
12	10.5	4.7	4.6	2.1	1.28	1.2	6

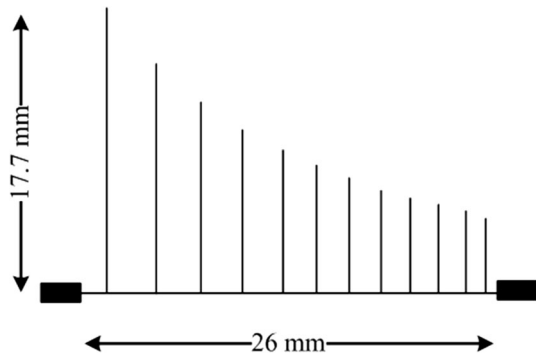


Fig. 5 Layout of the LPF with twelve T-shaped sections

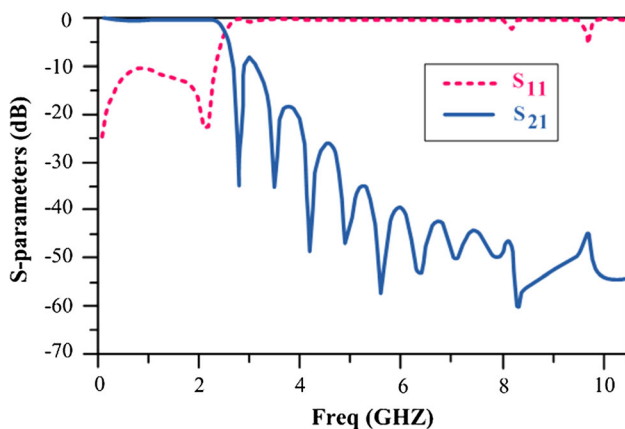


Fig. 6 EM simulation results of the LPF with twelve T-shaped sections

4th–15th harmonics (2.8–10.5 GHz). The first transmission zero of the designed LPF should be located at 2.8 GHz, so to have proper design the cut off frequency of filter should be at 2.5 GHz. The proposed LPF is created by cascading of 12 sections of T-shaped structure with characteristic

impedance of 142 Ω. Because the center frequency is 700 MHz, this filter must create 12 transmission zeros at multiples of the fundamental frequency, they could be located at:

$$2.8 + (m - 1) \times 0.7 \text{ GHz} \tag{17}$$

where $m = 1, 2, 3, \dots, 12$. Table 1 shows the calculated and extracted values from simulations for twelve-section LPF, with 142 Ω lines. The results show little difference between calculation values and simulations results, which confirm the validity of design process.

The Layout of the designed LPF with twelve T-shaped sections is shown in Fig. 5. The designed LPF is simulated by the advanced design system (ADS) software with RO4003 substrate ($\epsilon_r = 3.365$, thickness = 20 mil, loss tangent of 0.0033).

The dimensions of the designed filter with mentioned substrate is 17.7 mm × 26 mm ($0.353 \lambda_g \times 0.24 \lambda_g$). Unfortunately, this filter occupies large area.

The EM simulation results of the LPF with twelve T-shaped sections, is depicted in Fig. 6. As seen in this figure, the designed LPF creates twelve transmission zeros at desired frequencies with high attenuation levels, which features good harmonics suppression 4th–15th for the proposed divider.

As previously mentioned, the LPF with twelve T-shaped sections occupies large area; Therefore, to have both

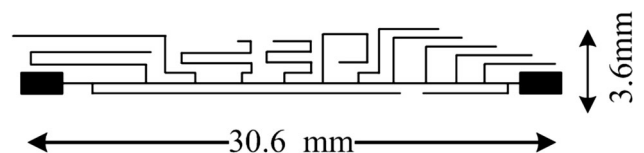


Fig. 7 Layout of the proposed LPF

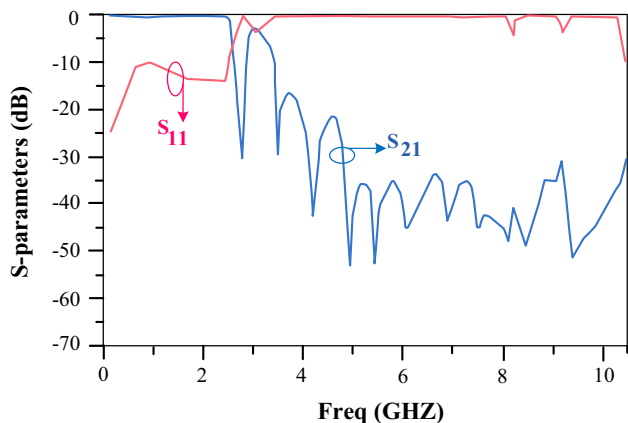


Fig. 8 Electromagnetic simulation results of the proposed LPF

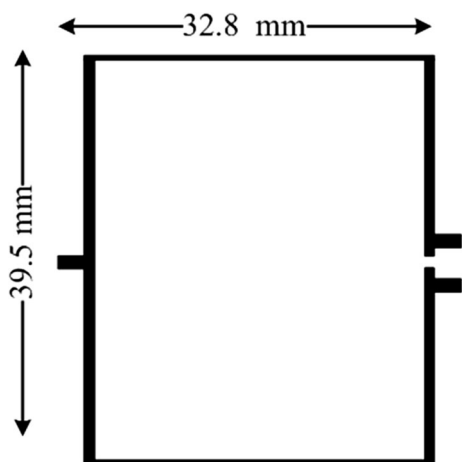


Fig. 9 Conventional Wilkinson divider at 700 MHz

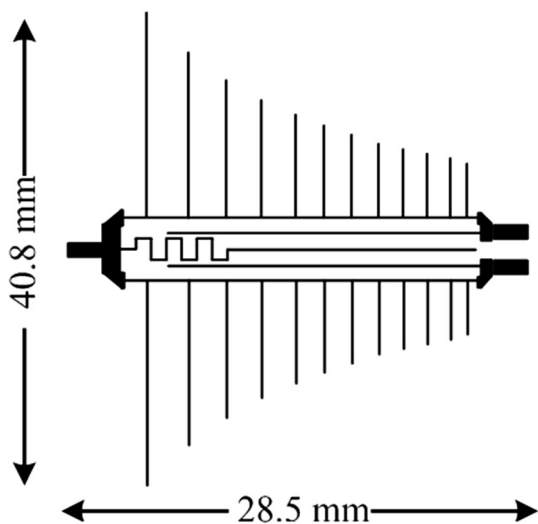


Fig. 10 Designed WPD using twelve T-shaped sections LPF

compact size and harmonics suppression properties, the proposed LPF is presented using bended stub lines as shown in Fig. 7.

In the proposed LPF, twelve T-shaped sections are bended, resulted in size reduction. The overall size of proposed LPF is only $3.6 \text{ mm} \times 30.6 \text{ mm}$ ($0.415 \lambda_g \times 0.048 \lambda_g$), which resulted in more than 75% size reduction, compared to the LPF with twelve T-shaped sections. The Electromagnetic (EM) simulation results of the designed LPF with twelve T-shaped sections, is shown in

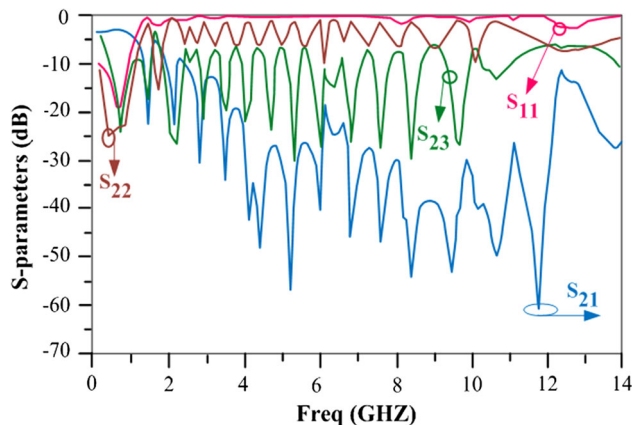


Fig. 11 EM simulation results of the designed WPD using twelve T-shaped sections LPF at 700 MHz

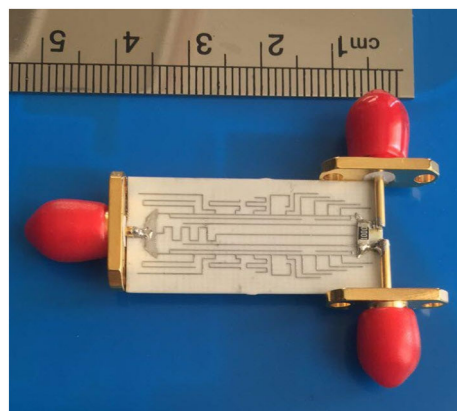
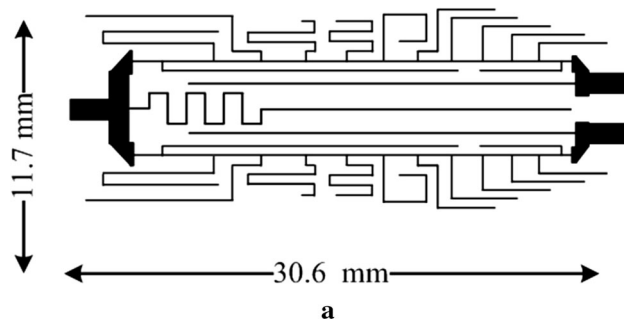


Fig. 12 a Layout and b fabricated photograph of the proposed WPD

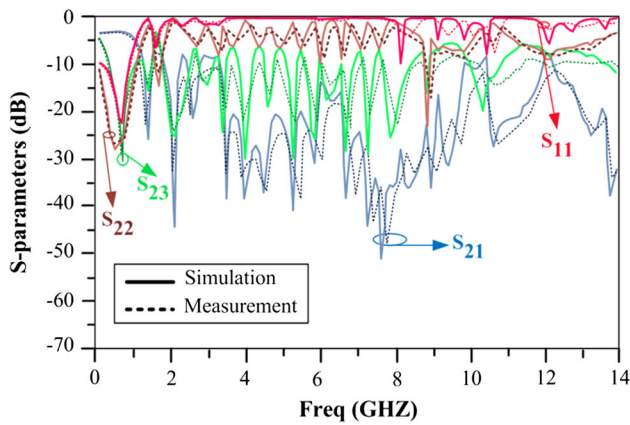


Fig. 13 EM simulation and measurement results of the proposed WPD

Fig. 8. The performance of the proposed filter is very good, which creates twelve transmission zeros at desired frequencies with high attenuation levels.

3.2 Design process of the proposed Wilkinson power divider

The layout of the conventional WPD is depicted in Fig. 9. The size of the conventional divider at 700 MHz with mentioned substrate (RO4003 with: $\epsilon_r = 3.365$, thickness = 20 mil, loss tangent of 0.0033) is 32.8 mm × 39.5 mm.

The layout of the Wilkinson divider using twelve T-shaped sections LPF is shown in Fig. 10. Three open stubs at three ports of the divider are applied to suppress lower harmonics (2nd and 3rd). Also, two LPFs which were introduced in the past section are applied as branch lines to suppress 4th to 15th harmonics.

The EM simulation results of this WPD are depicted in Fig. 11. The results show that the divider works correctly at 700 MHz and suppress the 2nd–15th harmonics with high levels of attenuation.

Unfortunately, this divider occupies large area. To reduce the large size of the presented divider, the applied twelve sections LPFs are replaced by proposed bended stubs LPFs, which described in the past section.

The Layout and fabricated photograph of the designed WPD are demonstrated in Figs. 12a, b, respectively. The size of the proposed divider is only 11.7 mm × 30.6 mm, which reduces the size of the divider more than 73% compared to the conventional WPD at 0.7 GHz. The electromagnetic (EM) simulation and measurement results of the designed WPD are depicted, in Fig. 13.

The results show that, the proposed divider successfully suppresses the 2nd–15th harmonics with high level of attenuations. A comparison between proposed power divider and other related works are summarized in Table 2. As result shows, the proposed power divider not only extremely reduces the circuit size but also has very good harmonics suppression compared to the reported works.

4 Conclusion

A compact LPF and a miniaturized, harmonics suppressed 0.7 GHz divider using open stubs are proposed in this paper. Three open stubs are used to suppress second and third harmonics at three ports of the divider and two novel 12-section low pass filters, based on aperiodic stubs, are applied to suppress 4th to 15th harmonics. The size of the proposed filter is very compact and results in a miniaturized power divider. The proposed divider not only has

Table 2 Performance comparison of the proposed WPD and other previous related works

References	Size reduction (%)	Harmonics suppression (dB)													
		2nd	3rd	4th	5th	6th	7th	8th	9th	10th	11th	12th	13th	14th	15th
[1]	–	40	40	40	–	–	–	–	–	–	–	–	–	–	–
[2]	71	58	46	30	32	41	57	33	39	21	10	10	–	–	–
[4]	–	71	77	36	26	34	–	–	–	–	–	–	–	–	–
[5]	35	–	45	–	43	–	–	–	–	–	–	–	–	–	–
[6]	29	–	53	25	56	20	–	–	–	–	–	–	–	–	–
[11]	70	8	32	10	12	–	–	–	–	–	–	–	–	–	–
[12]	39	26	25	–	–	–	–	–	–	–	–	–	–	–	–
[13]	–	18	15	–	–	–	–	–	–	–	–	–	–	–	–
[25]	63	13	29	32	34	–	–	–	–	–	–	–	–	–	–
This work	73	26	45	21	39	38	37	53	18	28	51	36	35	22	28

perfect harmonics suppression, but also extremely decreases the circuit size.

Acknowledgements The authors would like to thank the Kermanshah Branch, Islamic Azad University for the financial support of this research project.

References

- Cheng, K. K., & Ip, W. C. (2010). A novel power divider design with enhanced spurious suppression and simple structure. *IEEE Transactions on Microwave Theory and Techniques*, 58(12), 3903–3908.
- Hayati, M., Roshani, S., Roshani, S., & Shama, F. (2013). A novel miniaturized Wilkinson power divider with n th harmonic suppression. *Journal of Electromagnetic Waves and Applications*, 27(6), 726–735.
- Roshani, S., Siahkamari, P., & Siahkamari, H. (2017). Compact, harmonic suppressed Gysel power divider with plain structure. *Frequenz*, 71(5–6), 221–226.
- Hayati, M., Roshani, S., & Roshani, S. (2013). A simple Wilkinson power divider with harmonics suppression. *Electromagnetics*, 33(4), 332–340. <https://doi.org/10.1080/02726343.2013.777325>.
- Hayati, M., & Roshani, S. (2013). A novel Wilkinson power divider using open stubs for the suppression of harmonics. *ACES*, 28(6), 501–506. <https://doi.org/10.1080/09205071.2013.786204>.
- Hayati, M., Roshani, S., & Roshani, S. (2013). Miniaturized Wilkinson power divider with n th harmonic suppression using front coupled tapered CMRC. *ACES*, 28(3), 221–227.
- Heshmati, H., & Roshani, S. (2018). A miniaturized lowpass bandpass diplexer with high isolation. *AEU-International Journal of Electronics and Communications*, 87, 87–94.
- Rostami, P., & Roshani, S. (2018). A miniaturized dual band Wilkinson power divider using capacitor loaded transmission lines. *AEU-International Journal of Electronics and Communications*, 90, 63–68.
- Zhuang, Z., Wu, Y., & Liu, Y. (2017). Dual-band filtering out-of-phase balanced-to-single-ended power divider with enhanced bandwidth. *AEU-International Journal of Electronics and Communications*, 82, 341–345.
- Wang, X., Sakagami, I., Ma, Z., Mase, A., & Yoshikawa, M. (2015). Generalized, miniaturized, dual-band Wilkinson power divider with a parallel RLC circuit. *AEU-International Journal of Electronics and Communications*, 69(1), 418–423.
- Lin, C. M., Su, H. H., Chiu, J. C., & Wang, Y. H. (2007). Wilkinson power divider using microstrip EBG cells for the suppression of harmonics. *IEEE Microwave and Wireless Components Letters*, 17(10), 700–702.
- Zhang, F., & Li, C. F. (2008). Power divider with microstrip electromagnetic bandgap element for miniaturisation and harmonic rejection. *Electronics Letters*, 44(6), 422–424.
- Woo, D. J., & Lee, T. K. (2005). Suppression of harmonics in Wilkinson power divider using dual-band rejection by asymmetric DGS. *IEEE Transactions on Microwave Theory and Techniques*, 53(6), 2139–2144.
- Kazerouni, M., & Fartookzadeh, M. (2013). Design of a Two Octave Gysel power-divider using DGS and DMS. *Journal of Communication Engineering*, 2(2), 73–88.
- Huang, W., Liu, C., Yan, L., & Huang, K. (2010). A miniaturized dual-band power divider with harmonic suppression for GSM applications. *Journal of Electromagnetic Waves and Applications*, 24(1), 81–91.
- Gao, S. S., Sun, S., & Xiao, S. (2013). A novel wideband bandpass power divider with harmonic-suppressed ring resonator. *IEEE Microwave and Wireless Components Letters*, 23(3), 119–121.
- Song, K. (2015). Compact filtering power divider with high frequency selectivity and wide stopband using embedded dual-mode resonator. *Electronics Letters*, 51(6), 495–497.
- Song, K., Ren, X., Chen, F., & Fan, Y. (2013). Compact in-phase power divider integrated filtering response using spiral resonator. *IET Microwaves, Antennas and Propagation*, 8(4), 228–234.
- Ren, X., Song, K., Hu, B., & Chen, Q. (2014). Compact filtering power divider with good frequency selectivity and wide stopband based on composite right-/left-handed transmission lines. *Microwave and Optical Technology Letters*, 56(9), 2122–2125.
- Liu, H., Liu, C., Dai, X., & He, S. (2016). Design of novel compact dual-band filtering power divider using stepped-impedance resonators with high selectivity. *International Journal of RF and Microwave Computer-Aided Engineering*, 26(3), 262–267.
- Li, X., Shao, Z., Shen, M., & He, Z. (2016). High selectivity tunable filtering power divider based on liquid crystal technology for microwave applications. *Journal of Electromagnetic Waves and Applications*, 30(7), 825–833.
- Wang, X., Ohira, M., & Ma, Z. (2016). Coupled microstrip line Wilkinson power divider with open-stubs for compensation. *Electronics Letters*, 52(15), 1314–1316.
- Chen, C. J. (2014). Design of artificial transmission line and low-pass filter based on aperiodic stubs on a microstrip line. *IEEE Transactions on Components, Packaging and Manufacturing Technology*, 4(5), 922–928.
- Pozar, D. M. (2011). *Microwave engineering*. New York: Wiley.
- Wang, J., Ni, J., Guo, Y. X., & Fang, D. (2009). Miniaturized microstrip Wilkinson power divider with harmonic suppression. *IEEE Microwave and Wireless Components Letters*, 19(7), 440–442.
- Moradi, E., Moznebi, A. R., Afrooz, K., & Movahhedi, M. (2018). Gysel power divider with efficient second and third harmonic suppression using one resistor. *AEU-International Journal of Electronics and Communications*, 89, 116–122.
- Shahi, H., & Shamsi, H. (2017). Compact wideband Gysel power dividers with harmonic suppression and arbitrary power division ratios. *AEU-International Journal of Electronics and Communications*, 79, 16–25.
- Chen, C. J., Sung, C. H., & Su, Y. D. (2015). A multi-stub lowpass filter. *IEEE Microwave and Wireless Components Letters*, 25(8), 532–534.
- Rezaei, A., Noori, L., & Mohammadi, H. (2019). Miniaturized quad-channel microstrip diplexer with low insertion loss and wide stopband for multi-service wireless communication systems. *Wireless Networks*, 25(6), 2989–2996.
- Rezaei, A., & Noori, L. (2018). Miniaturized microstrip diplexer with high performance using a novel structure for wireless L-band applications. *Wireless Networks*. <https://doi.org/10.1007/s11276-018-1870-5>.
- Hikmaturokhman, A., Ramli, K., & Suryanegara, M. (2018). Spectrum Considerations for 5G in Indonesia. In *IEEE International Conference on ICT for Rural Development (IC-ICTRuDev)* (pp. 23–28).
- Liu, X., Jia, M., Na, Z., Lu, W., & Li, F. (2018). Multi-modal cooperative spectrum sensing based on Dempster–Shafer fusion in 5G-based cognitive radio. *IEEE Access*, 6, 199–208.
- Liu, X., Zhang, X., Jia, M., Fan, L., Lu, W., & Zhai, X. (2018). 5G-based green broadband communication system design with simultaneous wireless information and power transfer. *Physical Communication*, 25, 539–545.

34. Liu, X., Jia, M., Zhang, X., & Lu, W. (2018). A novel multi-channel internet of things based on dynamic spectrum sharing in 5G communication. *IEEE Internet of Things Journal*. <https://doi.org/10.1109/JIOT.2018.2847731>.
35. Ji, B., Song, K., Zhu, J., & Li, W. (2014). Efficient MAC protocol design and performance analysis for dense WLANs. *Wireless Networks*, 20(8), 2237–2254.
36. Ji, B., Zhu, J., Song, K., Huang, Y., & Yang, L. (2014). Performance analysis of femtocells network with co-channel interference. *Signal Processing*, 100, 32–41.
37. Ji, B., Xing, B., Song, K., Li, C., Wen, H., & Yang, L. (2018). Performance analysis of multihop relaying caching for internet of things under Nakagami channels. *Wireless Communications and Mobile Computing*. <https://doi.org/10.1155/2018/2437361>.

Publisher's Note Springer Nature remains neutral with regard to jurisdictional claims in published maps and institutional affiliations.



Sobhan Roshani received the B.Sc. degree in Electrical Engineering from Razi University, Kermanshah, Iran in 2010, M.Sc. degree in Electrical Engineering from Iran University of Science and Technology-IUST, Tehran, Iran in 2012 and Ph.D. in Electrical Engineering from Razi University in 2016. He has published more than 50 papers on International Journals and Conferences. His research interest includes switching power amplifiers, microwave

circuits, optimization and neural networks.



Saeed Roshani received the B.Sc. degree in Electrical Engineering from Razi University, Kermanshah, Iran in 2008, M.Sc. degree in Electrical Engineering from Shahed University, Tehran, Iran in 2011 and Ph.D. in Electrical Engineering from Razi University in 2015. He has published more than 50 papers in ISI Journals and Conferences and two books. His research interest includes the microwave and millimeter wave devices and circuits.